CHIN. PHYS. LETT. Vol. 34, No. 7 (2017) 074301

Source Range Estimation Based on Pulse Waveform Matching in a Slope Environment *

Zu-Yong Wu(吴祖勇)[1,2], Ren-He Zhang(张仁和)[2], Ji-Xing Qin(秦继兴)[2**],
Zhao-Hui Peng(彭朝晖)[2], Zhou Meng(孟洲)[1]

[1]*Academy of Ocean Science and Engineering, National University of Defense Technology, Changsha 410073*
[2]*State Key Laboratory of Acoustics, Institute of Acoustics, Chinese Academy of Sciences, Beijing 100190*

(Received 13 March 2017)

An approach of source range estimation in an ocean environment with sloping bottom is presented. The approach is based on pulse waveform correlation matching between the received and simulated signals. An acoustic propagation experiment is carried out in a slope environment. The pulse signal is received by the vertical line array, and the depth structure can be obtained. For the experimental data, the depth structures of pulse waveforms are different, which depends on the source range. For a source with unknown range, the depth structure of pulse waveform can be first obtained from the experimental data. Next, the depth structures of pulse waveforms in different ranges are numerically calculated. After the process of correlating the experimental and simulated signals, the range corresponding to the maximum value of the correlation coefficient is the estimated source range. For the explosive sources in the experiment with two depths, the mean relative errors of range estimation are both less than 7%.

PACS: 43.30.Dr, 43.60.Jn, 43.30.Zk DOI: 10.1088/0256-307X/34/7/074301

The transitional zone in the ocean is the channel connecting the shallow water and deep water. Acoustic problems in the transitional zone are important and have also received considerable attention in the underwater acoustics community recently. The sloping bottom widely exists in the transitional zone and the sound propagation is affected by it significantly. This study is directed against the source range estimation in the transitional zone.

The research about source range estimation is mainly concentrated in shallow water presently,[1−8] whereas it is insufficient in the transitional zone. The primary means applied to source range estimation in shallow water are match-field process (MFP), waveguide invariant process and warping transform process. Li *et al.*[1] applied the broadband MFP for source localization. The results show that the accuracy of the source localization is largely improved due to considering a sloped bottom. Cho *et al.*[2] unified the array/waveguide invariant approach to source range estimation, which is applied to a short-aperture vertical line array (VLA) in a fluctuating ocean environment over a one-day period. Results demonstrated the robustness of this approach. Qi *et al.*[3] proposed a frequency-warping operator for the autocorrelation function of the received signal in a range-independent shallow water waveguide. With a guide source providing the dispersive characteristics of the waveguide, the source range can be extracted from the relative delay time of the impulsive sequence using a single hydrophone. Based on the research of sound propagation from the shelf-break to deep water, Qin *et al.*[9] approximated the range of the air-gun source by comparing the relative energy level in the vertical direction between the experimental data and simulated results. Ballard[10] utilized the horizontal multipath caused by the horizontal refraction effect in the continental shelf environment to estimate source range. Heaney and Kuperman[11] located the source position with a small aperture vertical array. This method utilized the stability of early arriving wavefronts to determine the source range by matching wavefront arrival patterns.

In this Letter, an approach of source range estimation in an ocean environment with sloping bottom is proposed. The approach is based on pulse waveform correlation matching between the received and simulated signals. The data is acquired in an acoustic propagation experiment carried out in the transitional zone. Dispersion and multipath effects exist in the transmission path for the wideband pulse signal, thus the depth structures of received pulse waveforms are different when the range is changed. By correlating the experimental and simulated pulse signals with depth structure information, the source range is estimated, which corresponds to the maximum value of the correlation coefficient.

In September 2015, a sound propagation experiment was carried out in a transitional zone by the Institute of Acoustics, Chinese Academy of Sciences. The configuration of the experiment is shown in Fig. 1. The VLA is moored in a station with 1910-m water depth. The VLA is composed of 17 hydrophones spreading from 114 m to 1218 m with unequal space in depth. The sensitivity of the hydrophones is −170 dB. The Chinese R/V Shi Yan 1 starts from the receiver station and navigates along the upslope track. The wide band signals (WBSs) charged with 1000 g TNT are dropped almost equidistant from the ship

*Supported by the National Natural Science Foundation of China under Grant Nos 11434012 and 41561144006.
**Corresponding author. Email: qjx@mail.ioa.ac.cn

in the track. There are two kinds of nominal detonation depths (50 m and 200 m) for the WBSs. The sound speed profile (SSP) measured by expendable bathythermograph (XBT) is shown in Fig. 2(a), in which the sound channel axis is at the depth of about 1100 m. The bathymetry along the propagation track is given in Fig. 2(b), which changes from 1910 m at 0 km to 753 m at 58 km. The whole track is upslope overall and the incline angle is about 1.14°.

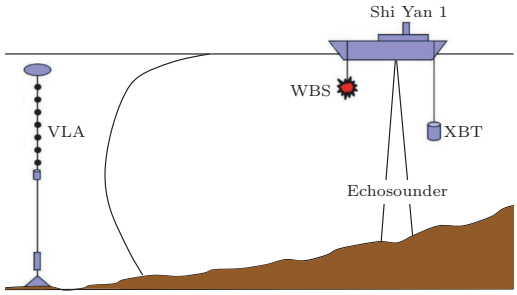

Fig. 1. Configuration of the experiment.

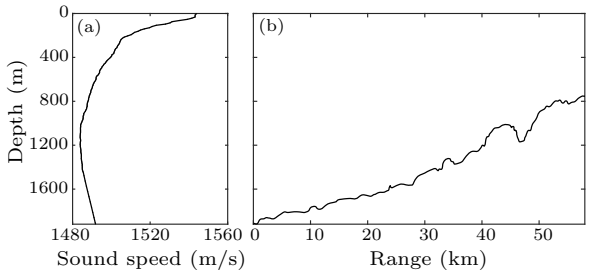

Fig. 2. Environmental information of the experiment. (a) Sound speed profile and (b) bathymetry along the propagation track.

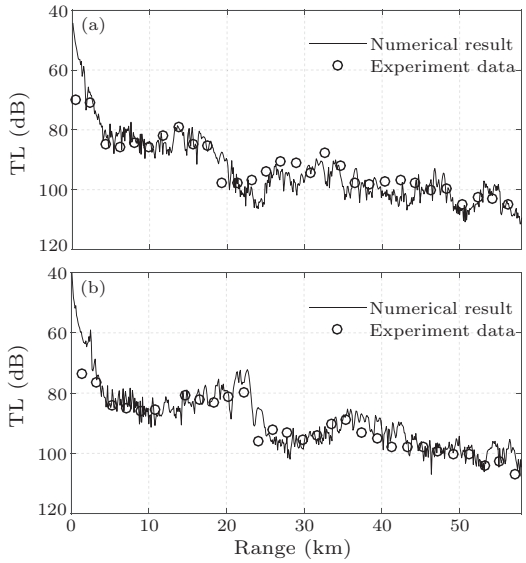

Fig. 3. Comparison of transmission losses. Here the receiver depth is 227 m, (a) the source depth is 50 m, and (b) the source depth is 200 m.

Next, we perform some simulations using the parabolic equation code RAM[12] to analyze and explain the experimental data. In the simulations, the measured SSP and bathymetry in Fig. 2 are used. The bottom is considered as a two-layer fluid model. The thickness of the sediment layer is 100 m, and the sound speed increases linearly from 1515 m/s to 1535 m/s. The density is 1.6 g/cm^3 and the attenuation coefficient is 0.3 dB/λ. In the semi-infinite basement, the sound speed is 1600 m/s, the density is 1.8 g/cm^3, and the attenuation coefficient is 0.3 dB/λ. The numerical transmission losses (TLs) are calculated at the central frequency of 300 Hz, and are averaged at seven frequency points within 1/3-octave bandwidth. When the receiver depth is 227 m, the comparisons of experimental and simulated TLs are shown in Fig. 3. Figure 3(a) shows the TLs comparison result for the source depth of 50 m, and Fig. 3(b) shows the comparison result for the source depth of 200 m. We can see that the TLs calculated by numerical model and from experimental data agree well.

Assuming the radiated source signal form as $f(t)$, with a frequency spectrum $S(\omega)$, the pressure in the time domain at the receiver point (r, z) can be obtained via a Fourier transform of the frequency-domain solution of wave equation as[13]

$$p(r,z,t) = \frac{1}{2\pi}\int_{-\infty}^{\infty} S(\omega)g(r,z,\omega)e^{-i\omega t}d\omega, \quad (1)$$

where $g(r, z, \omega)$ is the spatial transfer function. Within the concerned frequency bandwidth, we replace Eq. (1) by

$$p(r,z,t) = \frac{1}{2\pi}\int_{-\omega_{\max}}^{\omega_{\max}} S(\omega)g(r,z,\omega)e^{-i\omega t}d\omega. \quad (2)$$

Next, we choose the source frequency centered at 300 Hz and with a 50 Hz bandwidth, corresponding to frequency spectrum as follows:

$$S(\omega) = \begin{cases} 1, & 275\,\text{Hz} \leqslant \omega/2\pi \leqslant 325\,\text{Hz}, \\ 0, & \text{Others}. \end{cases} \quad (3)$$

When the source explodes at 200 m depth and is 5.2 km away from the VLA, the signals received in the experiment and the numerical results are shown in Fig. 4. Figure 4(a) shows the experimental results, which are fitted by a band pass filter as mentioned above, and the numerical results calculated in the same situation are shown in Fig. 4(b).

Figure 5 shows the signals received in the experiment and the numerical results when the source explodes at 200 m depth and is 24.1 km away from the VLA. Figure 5(a) shows the experimental results, which are fitted by a band pass filter as mentioned above, and the numerical results calculated in the same situation is shown in Fig. 5(b).

From the above comparisons between the experimental and numerical pulse waveforms, we observe that the depth structures agree well. Moreover, the depth structures of pulse waveforms are different when the source ranges are changed. Accordingly, we can estimate the source range through matching the depth structure of pulse waveform.

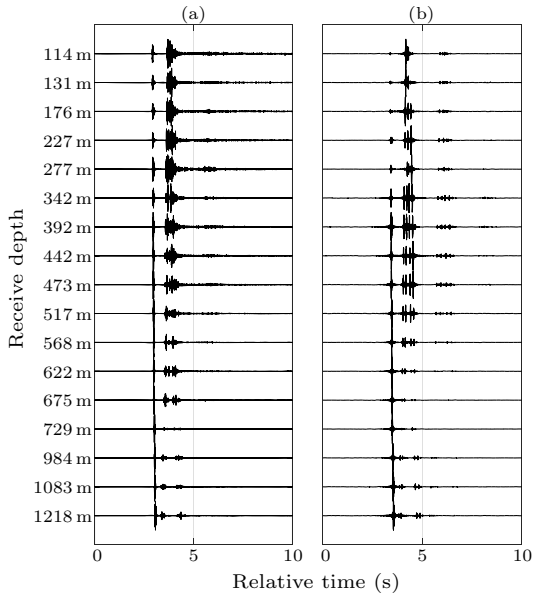

Fig. 4. Received pulse waveforms for the 200-m source depth and 5.2-km distance. (a) Experimental results, (b) numerical results.

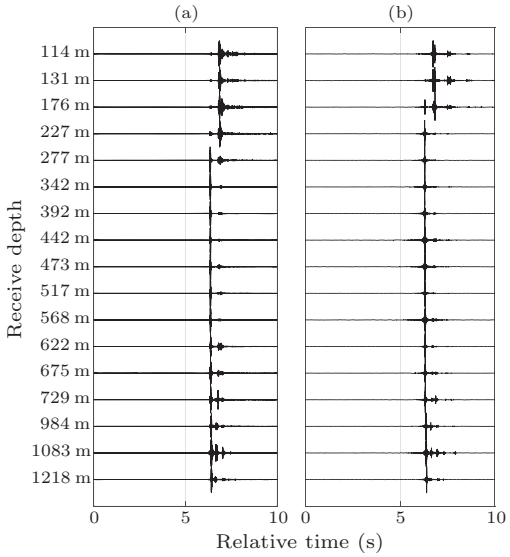

Fig. 5. Received pulse waveforms for the 200-m source depth and 24.1-km distance. (a) Experimental results, (b) numerical results.

When the range between the source and receiver is r, the signal recording time is T, and the signal expression is $s(r,t)$, we define the received signals as follows:

$$x(r,t) = \begin{cases} s(r,t), & 0 \leqslant t < T, \\ 0, & \text{Others}. \end{cases} \tag{4}$$

We have known that the depth structures of pulse waveforms are different when the source range varies. If we transform the two-dimensional pulse waveform (depth and temporal distribution) into one-dimensional (temporal distribution), we will obtain a long-time pulse sequence and each one-dimensional pulse structure should correspond to a unique source range. According to this characteristic, we delay and normalize the pulse signals recorded by all the channels, then superpose all delayed signals and suppose that all signals are received by the first channel. After that, we can obtain a long-time pulse sequence, and the output is given by

$$S(r,t) = \sum_{n=1}^{M} \frac{x_n(r, t-(n-1)\times T)}{|x_n|_{\max}}, \tag{5}$$

where $x_n(r,t)$ is the signal output of the nth channel, $|x_n|_{\max}$ is the maximum absolute value of the nth channel, and M is the total of array elements.

When the source range is unknown, we can estimate it by the method as follows: First, process the experimental data through Eqs. (4) and (5) and denote the processed signal by $S_{\exp}(r,t)$. Then suppose that the source range is r' and obtain the numerical data. We also process the simulated data by Eqs. (4) and (5) and denote the processed signal by $S_{\text{cal}}(r',t)$. We next extract the envelopes of experimental and numerical results, denoted by $\tilde{S}_{\exp}(r,t)$ and $\tilde{S}_{\text{cal}}(r',t)$, respectively. Then the cross-correlation coefficients between them are calculated by

$$\rho(r,r') = \max_{\tau} \frac{\int_{-\infty}^{+\infty} \tilde{S}_{\exp}(r,t)\tilde{S}^{*}_{\text{cal}}(r',t-\tau)dt}{\sqrt{\int_{-\infty}^{+\infty} \tilde{S}^{2}_{\exp}(r,t)dt \int_{-\infty}^{+\infty} \tilde{S}^{2}_{\text{cal}}(r',t)dt}}, \tag{6}$$

where $*$ is the complex conjugate operation. The cross-correlation coefficient is defined as the maximum of normalized delay correlation algorithm. We can obtain cross-correlation coefficient $\rho(r,r')$ under different ranges of r'. The range corresponding to the maximum value of the correlation coefficient is the estimated source range.

When the source depth is 200 m and the range is 5.2 km, after correlated process of the experimental data and the numerical data, the cross-correlation coefficient versus the source range is shown in Fig. 6. The range corresponding to the maximum value of the correlation coefficient is 5.3 km, which is the estimated source range.

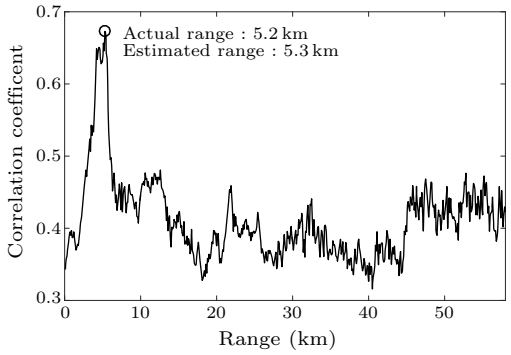

Fig. 6. Cross-correlation coefficient versus source range for the 200-m source depth and 5.2-km actual source range.

Applying the algorithm to all the experimental data in the propagation track, we present the results in Figs. 7 and 8. When the source depth is 200 m, the

results of range estimation are shown in Fig. 7 and the mean relative error is 5.21%. When the source depth is 50 m, the results of range estimation are shown in Fig. 8 and the mean relative error is 6.12%. The results show that this algorithm is effective for source range estimation, except individual data for the 200-m source depth. Due to the errors of bottom parameters in the complicated environment with a sloped bottom, the range estimation would have bad performance in some special ranges.

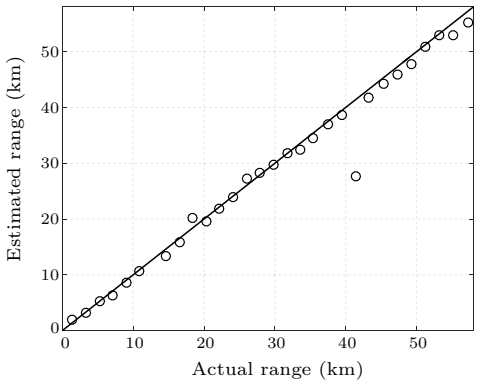

Fig. 7. Estimated source range in the propagation track when the source depth is 200 m.

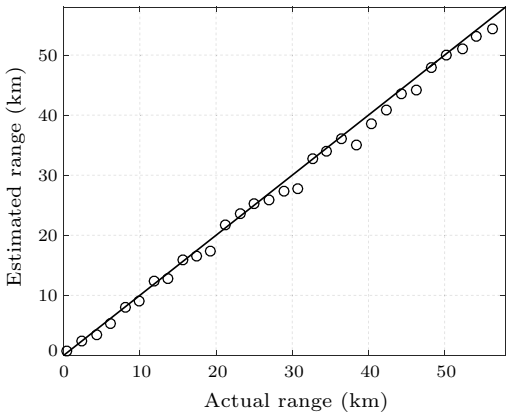

Fig. 8. Estimated source range in the propagation track when the source depth is 50 m.

In summary, the sound propagation is affected by the bottom significantly in a sloped environment, which causes the received pulse signal to be relatively complicated. For experimental data, the depth structure of pulse waveform can be obtained by a VLA and we observe that the depth structure of pulse waveform is different when the source range changes. Consequently, a source range estimation method based on matching the depth structure of pulse waveform is proposed. We delay the pulse signals recorded by all the channels, then superpose all delayed signals and suppose that all signals are received by the first channel. This step transforms the two-dimensional pulse waveform (depth and temporal distribution) into one-dimensional (temporal distribution), which not only reserves the distribution structure of pulse waveform but also provides more information for range estimation. For different source depths, the mean relative errors for range estimation are all below 7%, which show that this algorithm is effective.

We thank all the staff in the marine comprehensive experiment in 2015.

References

[1] Li Z L, Zhang R H, Yan J, Peng Z H and Li F H 2003 *Acta Acust.* **28** 425
[2] Cho Chomgun, Song H C and Hodgkiss W S 2016 *J. Acoust. Soc. Am.* **139** 63
[3] Qi Y B, Zhou S H, Zhang R H and Ren Y 2015 *Acta Phys. Sin.* **64** 074301 (in Chinese)
[4] Qi Y B, Zhou S H, Ren Y, Liu J J, Wang D J and Feng X Q 2015 *Acta Acust.* **40** 144
[5] Thode A M 2000 *J. Acoust. Soc. Am.* **108** 1582
[6] Yao M J, Ma L, Lu L C and Guo S M 2014 *Acta Acust.* **39** 685
[7] Zhu L M, Li F H, Sun M and Chen D S 2015 *Acta Phys. Sin.* **64** 154303 (in Chinese)
[8] Wang D, Guo L H, Liu J J and Qi Y B 2016 *Acta Phys. Sin.* **65** 104302 (in Chinese)
[9] Qin J X, Zhang R H, Luo W Y, Peng Z H, Liu J J and Wang D J 2014 *Sci. Chin.: Phys. Mech. Astron.* **57** 1031
[10] Ballard M S 2013 *J. Acoust. Soc. Am.* **134** EL340
[11] Heaney K D and Kuperman W A 1998 *J. Acoust. Soc. Am.* **104** 2149
[12] Collins M D 1994 *J. Acoust. Soc. Am.* **96** 382
[13] Jensen F B, Kuperman W A, Porter M B and Schmidt H 2011 *Computational Ocean Acoustics* 2nd edn (New York: Springer)